Tortajada-Genaro, LA.; Borrás García, EM.; Muñoz, A. (2013). Gas-phase and particulate products from the atmospheric degradation of an isoxazole fungicide. Chemosphere. 92(8):1035-1041. doi:10.1016/j.chemosphere.2013.03.041.

Gas-Phase and Particulate Products from the Atmospheric Degradation of an Isoxazole Fungicide

Luis Antonio Tortajada-Genaro†*, Esther Borrás ‡, Amalia Muñoz‡

† Instituto de Reconocimiento Molecular y Desarrollo Tecnológico-Departamento Química, Universitat Politècnica de València, Spain.*

‡ Centro de Estudios Ambientales del Mediterráneo (Fundación CEAM), Spain

*** Corresponding author**

Luis Antonio Tortajada Genaro

Departamento de Química-IDM

Universitat Politécnica de València

Camí de Vera s/n, 14,

46022, Valencia – Spain

e-mail: luitorge@qim.upv.es

Phone: +0034 96 38773423

Fax: +0034 963879349

ABSTRACT: The isoxazole structure is present in several pesticides. However, there is a lack of information about its degradation products after the release to the atmosphere. The main atmospheric reactions of hymexazol (5-methylisoxazol-3-ol), selected as representative model, were investigated at a large outdoor simulation chamber. The predominant products of atmospheric degradations were gaseous nitrogen derivates (nitric acid, nitrogen dioxide, nitrogen oxide, nitrous acid, and peroxyacetylnitrate), ozone, and small oxygenated compounds (formic acid, formaldehyde, and methylglyoxal). The aerosol yields were lower than 5 %, and an OH rate-dependence was observed in the nucleation, particle growth, and size distribution. Also, the chemical composition of minor multi-oxygenated products was studied for OH-photo-oxidations. More than 20 products were detected in the gas or particulate phase. The most abundant were heterocyclic cleavage products with C4-chain and oxygenated moieties at positions 1 and 3, such as 3,4-dioxobutanoic acid, 3-oxobutanoic acid, and 3-oxobutanal. The suggested reaction pathway is the opening of heterocycle ring by the cleavage of N-O bond and C-N bond, releasing nitrogen oxides.

Keywords: isoxazole, pesticide, hymexazol, aerosol, photo-oxidation, reaction mechanism

1. INTRODUCTION

The isoxazole structure is a 1,2-azol, five-membered aromatic heterocyclic with an oxygen and a nitrogen. These compounds have a wide range of applications, including fungicides, insecticides, herbicides and drugs. Examples of aproved pesticides in Europe are hymexazol, isoxaben and isoflutole. Other compounds are drazoxolon, isouron, isoxathion (not approved), topramezone (pending) or isoxachlortole (not registered in Europe). The release of pesticides based on isoxazole structure to the environment is produced during the manipulation, application and post-application, being the volatilization from the treated surface the most important input into the troposphere (Van den Berg et al., 1999).

The information about the atmospheric behavior of isoxazoles (as many pesticides and heterocycle compounds) is quite scarce. As other semi-volatile organic compounds (SVOCs) in the atmosphere, isoxazoles are distributed between gas and particle phase (Atkinson et al., 1999). An oxidative degradation is also produced reducing its concentration, but new products are also formed. These secondary pollutants, called residues, include gaseous or condensed compounds with a different atmospheric residence time, and sometimes worse toxicity than the original molecule. However, experimental results about pesticides have been reported only for a lower number of products (Atkinson et al., 1999; Le Person et al., 2007; FOCUS Working Group, 2008). In order to get a comprehensive overview of their atmospheric fate, both their gas and particulate reactivity must to be taken in consideration. For that, the use of atmospheric simulation chambers solves some of the difficulties appeared to carry out realistic laboratory studies (Finlayson-Pitts and Pitts, 2000; Feigenbrugel et al., 2006). These full-equipped facilities have allowed the examination of pollutant degradations under atmospheric controlled conditions, such furan, thiophene or pyrrole - aromatic

69 cycles with one heteroatom - (Atkinson et al., 1983; Atkinson et al., 1984; Bierbach et
70 al., 1992; Cabañas et al., 2004; Gómez-Álvarez et al., 2009) or pesticides (LePerson et
71 al., 2007, Muñoz et al., 2012).

72 An important isoxazole systemic fungicide is 5-methylisoxazol-3-ol, named
73 hymexazol being used to control diseases caused by soil-borne pathogens and a plant
74 growth stimulant. In the present study, this compound has been selected as model of
75 isoxazole reactivity due to its high input in the atmosphere: relatively high volatility
76 (vapor pressure of 182 mPa at 25 ºC) and high use. Since its entry onto the market in the
77 seventies, the number of application has increased – e.g. rice, vegetable, tobacco,
78 tomato, and cucumber crops -. In fact, hymexazol is the only registered fungicide that
79 controls both *Aphanomyces* and *Pythium*, and thus is used worldwide as a standard
80 treatment for sugar beet seed (Payne and Williams, 1990).

81 A previous study performed in our atmospheric chamber was focused on the
82 general description of the hymexazol degradation and the contribution of each
83 atmospheric reaction was compared with other pesticides (Vera et al., 2011). The main
84 aim of the present study is the analysis of its OH-degradation products. Measurements,
85 based on specific instruments and chromatographic techniques, provide information in
86 regard to the composition and the concentration of formed products in the gas phase as
87 well as particulate phase, contributing to the elucidation of the degradation pathway and
88 the evaluation of its environmental impact.

89 ## 2. EXPERIMENTAL SECTION

90 The experiments were carried out in the EUPHORE photoreactors (Valencia,
91 Spain). These chambers consist of two half spherical fluoropolymeric bags, each one of
92 200 m^3 with integrated measuring systems for monitoring precursor species, pressure,
93 humidity, temperature, and reaction products (Borrás and Tortajada-Genaro2012a). A

white-type mirror system (path length of 553.5 m) coupled to a Fourier Transform Infrared spectrometer with MCT detector (NICOLET Magna 550) was used for recording concentrations of major gaseous products. Specific monitors were integrated for measuring NO, NO_2, NO_x and O_3, free of interferences. Aerosol mass concentration was measured with a scanning mobility particle sizer (SMPS).

The chamber set-up or background measurements, see Table 1, were performed filling the photoreactor with air from a purification system. In experiments type A and B, the photoreactor was left without/with sunlight radiation, to reproduce the same conditions as for ozonolysis and photo-exposed reactions, respectively. In experiment type C, the photoreactor was left in darkness, with an inorganic seeds addition (acidified ammonium sulfate solution of 0.06 M) to establish the aerosol wall losses. Moreover, hymexazol was injected via heated air stream to the closed chamber in order to assure the absence of electrostatic effects with chamber walls. The formation of volatile (background upper limits: O_3 17 ± 1 μg m^{-3}, NO 0.4 ± 0.1 μg m^{-3}; NO_2 5.3 ± 0.5 μg m^{-3}; HONO 2.9 ± 0.2 μg m^{-3}, HNO_3 1.3 ± 0.1 μg m^{-3}) and particle artifacts (background upper limit: 1 μg m^{-3}) were negligible.

The oxidation experiments consisted of the degradation under dry conditions (<2% RH, 295-298 K) in the absence of inorganic seed aerosol (Table 1). Regarding the induced photolysis, cyclohexane was added via sprayer as scavenger of OH radicals. For the ozonolysis, ozone was produced by passing oxygen through a photo-generator (λ = 280 – 320 nm). For photo-oxidation experiments, hydrogen peroxide was introduced by a sprayer, and HONO was generated by a liquid-phase reaction between a 0.5% $NaNO_2$ solution and a 30% H_2SO_4 solution and transferred via a stream of purified air. Later, all the reactants were mixed for 10 min before exposing them to sunlight ($J_{NO2} \approx 7\times10^{-3}$ s^{-1}) or kept in darkness for ozone experiment. The onset of

aerosol formation (0.01 μg m^{-3}, 60 particles cm^{-3}) was considered to occur when the first significant particle concentration was registered ($3\sigma_{background}$). The specific dilution process was determined using SF_6 as a tracer being 6.5×10^{-6} s^{-1} the average rate. Finally, the average OH concentrations present in the smog chamber during the photo-oxidation reactions were calculated from the second-order decay of hymexazol (k_{OH} = (4.4 ± 0.8) × 10^{-12} cm^3 $molecule^{-1}$ s^{-1}). The estimated concentration of OH radical was 2 × 10^6 radicals cm^{-3} for experiment in the absence of NO_x and 8.8 × 10^6 radicals cm^{-3} in the presence of low-NO_x.

For fingerprint analysis, gaseous products were sampled with C18 cartridges during reaction, under a flow rate of 1 L min^{-1} for 0.5 h. Particles were collected at maximum aerosol formation, under a flow rate of 80 L min^{-1} for 1 h, on quartz fiber filters that had been pre-baked at 500 ºC for 12 h. A blank investigation of cartridges and filters was done to identify possible artifact formation and no compounds or artifacts were observed. The analysis of multi-oxygenated compounds by gas chromatography-mass spectrometry technique was similar to describe in reference (Borrás and Tortajada-Genaro, 2012b). The specific protocol has been included in *Supplementary Information*.

3. RESULTS AND DISCUSSION

3.1 Hymexazol consumption and gaseous products

The first step was a theoretical study of isoxazole molecule reactivity based upon the structure-activity relationship (SAR) methods developed by Kwok and Atkinson, 1995. The molecular modeling indicated a low degradation rate by photolysis and ozonolysis reactions but the OH-nucleophilic attack is favored and directed to certain positions with more positive charge density. The kinetic rate constant, k_{OH}

143 ($cm^3molecule^{-1}s^{-1}$) for hydrogenated isoxazole ring was 9.1×10^{-12} $cm^3molecule^{-1}s^{-1}$.
144 The theoretical OH kinetic rate constant of other isoxazole rings changed depending on
145 substituents groups. Examples of rate constants are 6×10^{-12}, 200×10^{-12} and 204×10^{-12}
146 for isoxaflutole, hymexazol and isoxaben – pesticides allowed in Europe -, respectively.
147 Then, the atmospheric formation of oxygenated degradation products from isoxazoles is
148 expected to be important.

149 The following step was focused on the atmospheric reactivity of hymexazol as a
150 model compound, measured in simulation chamber. Its consumption was calculated
151 from the experimental reaction profiles (see *Supplementary Information*). The
152 degradation percentages from photo-oxidations were 28.8 % in the absence of NO_x, and
153 50.0 % in the presence of NO_x, being substantially higher than those from photolysis
154 (3.0 %) and ozonolysis (4.0 %). The experimental consumptions of hymexazol, under
155 both OH-photo-oxidations, were between 26 and 45-fold lower than estimated by SAR
156 method and measured OH concentrations ($2 \times 10^6 – 8.8 \times 10^6$ molecules cm^{-3}). The
157 results indicated that SAR method underestimate the rate constant for hymexazol. Other
158 researchers have also observed these discrepancies between theoretical and
159 experimental rate constants if some of the subsequent reactions of the precursor and
160 products formed are not considered (Mereau et al., 2003).

161 Different gaseous products were observed as function of the degradation modes
162 and their maximum reaction yields were calculated at steady state (Table 2). The main
163 products from OH photo-oxidation reaction were ozone, nitric acid, nitrogen dioxide,
164 nitrogen oxide, and formic acid. Other gases were formaldehyde, nitrous acid,
165 methylglyoxal, and peroxyacetylnitrate (PAN). Short chain oxygenated products, such
166 as formaldehyde, formic acid and methylglyoxal were produced as result of the
167 oxidative breakdown of C-C bonds. The amount produced of NO_2, NO, HNO_3, and

PAN was interpreted as a loss of N-atom after OH attack, since these compounds were determined up to background levels. The cleavage of isoxazole ring first produce NO_x and the rest of N-containing products are formed from further reactions. In the presence of NO_x, HNO_3 is also produced by the reaction between the initial NO_2 and OH, explaining its high observed concentration and NO_2 levels. This assumption for ring-cleavage was corroborated comparing the OH-photo-oxidations of other nitro-compounds, concluding that hymexazol provides higher yields of NO_x, HNO_3 and PAN than ortho-nitrophenols (Bejan et al., 2006). Although the photolysis and ozonolysis reaction rates were almost negligible low, the results pointed out a relevant formation of O_3 and NO_2 compared to the background experiments, confirming that the loss of nitrogen atom from heterocycle is an important process. In case of photolysis, the equilibrium between NO and NO_2 produces oxygen radical and this radical reacted with O_2 to form O_3. In case of ozonolysis, the direct release of NO_2 or the reaction between NO and O_3 could promote the increase of NO_2 concentration (Finlayson-Pitts and Pitts, 2000).

Figure 1 shows the products profiles for both OH-photo-oxidations. A delay about 30 min after sunlight exposure was observed for the reaction in absence of NO_x, being 5 h the reaction time for reaching the maximum hymexazol consumption. Under the addition of HONO, products were formed immediately after the exposure to sunlight radiation with a lower reaction time (3.5 h). This behavior has been observed for other photo-oxidations, indicating a higher reactivity in high polluted locations and associated to the rate of OH formation (HONO >> H_2O_2) (Borrás and Tortajada-Genaro 2012a). Furthermore, the reactivity could increases due to other competitive oxidation channels (i.e. reaction of hymexazol with HO_2 radical).

3.2 Formation of particle matter

A detectable amount of particulate matter was obtained in all experiments, compared to chamber control experiments. The concentrations were 3.4, 2.9, 28, and 40 μg m^{-3} for photolysis, ozonolysis, NO_x-absence photo-oxidation, and NO_x-presence photo-oxidation, respectively. The aerosol yields (Y), calculated from the maximum aerosol mass concentration formed (M_o) and the mass concentration of hymexazol reacted (ΔHC), were lower than 5 %. The aerosol yields were similar to other heterocycles such as furan (2 - 7%), 2-methylfuran (5.5 %), and 3-methylfuran (8.5%) (Gómez-Álvarez et al., 2009) or benzene (Borrás and Tortajada-Genaro, 2012a); but lower than substituted-aromatic compounds such as toluene (33%) (Borrás and Tortajada-Genaro, 2012b) and xylenes (6 – 38%; Ng et al., 2007). The results obtained in the present study, indicated that the atmospheric degradation of isoxazole ring mainly lead the formation products with a high vapor pressure (volatiles products). Nevertheless, a higher aerosol formation is expected in the atmosphere, associated to an early gas-condensed phase partitioning of semi-volatile products on the ambient particles (Ng et al., 2007) or at lower temperatures.

Figure 2 illustrates aerosol profiles for both OH-photo-oxidations. The first observation was the rapid OH generation from HONO photolysis that promoted an immediate particulate matter formation. In NO_x-absence conditions, the beginning of nucleation required a sunlight exposure of 1 h (30 min later than first gaseous products). The existence of a delay is due to an induction period, where condensable compounds reach their saturation point (Ng et al., 2007). Secondly, the aerosol growth was studied, calculating the curves of the aerosol mass concentration (ΔM_o) as a function of the hymexazol reacted (ΔHC). A strong linear correlation ($R^2 > 0.95$) was observed with slopes 0.0473 ($\overline{Y} = 4.73 \pm 0.23$ %) and 0.0481 ($\overline{Y} = 4.81 \pm 0.24$ %) for the absence and

217 the presence of NO_x, respectively. The maximum formation was reached 5 h and 3.5 h
218 after the start of nucleation for the NO_x-absence and presence, respectively.
219 The particle size distributions versus time were also studied (inserts of Figure 2).
220 In both OH-photo-oxidations, an initial growth controlled by condensation or
221 homogeneous/binary nucleation process was observed. Then, the growth continued and
222 particle distribution moved to larger sizes, showing a bimodal distribution due to the
223 coagulation of particles and condensation of semi-volatile compounds on their surface.
224 This behavior is most evident in the absence of NO_x conditions, owing to the slowest
225 OH production. Finally, when the steady state was reached, the particle size remained
226 constant.

227 ### 3.3 Other carbon-containing degradation products

228 The atmospheric oxidation of semi-volatile compounds generates multi-
229 oxygenated products. For that, their determination by GC-MS technique was applied to
230 gas-phase and particulate samples collected during reaction. A typical chromatogram of
231 a high NO_x photo-oxidation gaseous sample analyzed in the electron ionization mode is
232 shown in Figure 3. A total of 23 products, listed in *Supplementary Information*, were
233 found. Most molecules were detected in both OH-photo-oxidant conditions and both
234 gaseous and particle phases.
235 The most abundant products were C4-ring-cleavage compounds with
236 oxygenated moieties at positions 1 and 3. They included 3,4-dioxobutanoic acid, 3-
237 oxobutanoic acid, 3-hydroxybutanoic acid, 3-oxobutanal, 4-hydroxybutan-2-one, and 2-
238 oxobutanedioic acid. Other nitro/nitroso substituted compounds were tentatively
239 identified, such as 4,4-dihydroxy-4-nitrosobutan-2-one and 1-nitrosobuta-1,3-diene-1,3-
240 diol. Short chain compounds were detected such as 2-oxopropanoic acid, acetone,
241 acetaldehyde, or hydroxyacetone. Glyoxal and methyl-glyoxal were detected in both gas

and particulate phases. Only two ring-retaining products were detected at trace levels and tentatively identified as 5-(hydroxymethyl)isoxazol-3-ol and 3-hydroxyisoxazole-5-carbaldehyde.

Moreover the identification of new identified carbon-containing degradation products appears on *Supplementary Information*. We describe the interpretation of mass spectrum for three relevant tentative products obtained by GC-MS in the EI mode. These products are representatives of the main reaction pathway proposed.

3.4 Degradation pathways of OH-photo-oxidations

The reaction of OH radical with isoxazole takes place via: OH addition and H-atom abstraction, see *Supplementary Information*. The theoretical reactivity model suggested that a double bond OH addition (10^{-14}-10^{-10} cm^3 $molecule^{-1}$ s^{-1}) prevails against the H-abstraction (10^{-17}-10^{-14} cm^3 $molecule^{-1}$ s^{-1}). The proposed OH-attack proceeds through a pre-reactive complex, the OH radical forms a hydrogen bond with the heterocycle π-system, as being suggested in the literature (Dillon et al., 2012). The further adduct radicals are resonance-stabilized, since there is a delocalization across the ring. However, the specific orientation of the addition and the ring-cleavage mechanism should depend on the ring moieties.

The OH-attack to hymexazol followed by C-C bond fission was proposed in our previous study, according to the general reaction pathway for 5-membered oxygen-containing ring alkoxy radicals (Mellouki et al., 2003). However, the expected main product (N-(acetyloxy)-2-oxoethanimidic acid), was not detected. Other results of present study, such as the formation of nitrogen oxides and the detection of several structurally defined carbon-containing products deserve special emphasis to propose an alternative and experimentally supported reaction pathway. The nucleophilic attack, based on the positive charge density of hymexazol, is oriented to C-3 (hydroxyl group)

267 and, to a lesser extent, C-5 (methyl group), rather than C-4 (non substitutions).
268 Consecutive reactions lead to the cleavage of the ring, the loss of nitrogen oxides, and
269 the formation of 1,3-oxygenated C4-products, e.g. 3-oxobutanal. This ring-cleavage is
270 entropically favored for the formation of new gas molecules and has been described for
271 other aromatic systems (Baltaretu et al., 2009). Moreover, after the aromatic π-system is
272 lost, the cleavage of N-O bond (~220 kJ mol^{-1}) and C-N bond (~300 kJ mol^{-1}) is more
273 favorable than the cleavage of C-O bond (~360 kJ mol^{-1}) or C-C bonds (~350 kJ mol^{-1})
274 (Finlayson-Pitts and Pitts, 2000). Further degradation of C4-products leads to the
275 formation of small multi-oxygenated products, e.g. hydroxyacetone. These products are
276 commonly identified in the photo-oxidations of unsaturated hydrocarbons or aromatic
277 compounds (Borrás and Tortajada-Genaro, 2012a; 2012b). Although, the proposed
278 pathway is consistent with the reaction products detected, the lack of other experimental
279 data introduces an uncertainty about the intermediates.

280 On the other hand, a high barrier for the exothermic H-abstraction is expected,
281 because the reaction changes the π-system of the ring as it occurs on other aromatic
282 systems (Borrás and Tortajada-Genaro, 2012a), or pyrrole (Dillon et al., 2012).
283 However, the H-abstraction from the methyl group of hymexazol is a relevant reaction
284 as it occurs on toluene (Baltaretu et al., 2009). The detection of 3,4-dioxobutanoic acid
285 and 2-oxobutanedioic acid (oxygenated group at position 1) is an experimental evidence
286 that supports this reaction pathway.

287 ## 4. ATMOSPHERIC IMPLICATIONS

288 The contamination with pesticides presents an important environmental and
289 toxicological concern (Atkinson et al., 1999). Regarding the atmospheric hazards
290 associated with the extensive use of pesticides, knowledge of the specific degradation

291 products is necessary in order to assess their potential impact. So, the design and
292 selection between molecules with similar action should be carefully performed
293 according to their persistence properties. The isoxazole family is an example of
294 compounds which number of derivatives and applications is continuously increasing,
295 but their atmospheric chemical behavior is practically unknown. The present study,
296 based on the use of photochemical reactors, contributes in this area providing useful
297 data about degradation products and yields. Extrapolating the results of hymexazol
298 degradation – simulating atmospheric concentrations and isolating of other effects as
299 dispersion and transport –, we can hypothesize that isoxazole compounds are labile to
300 OH-photo-oxidation and partially persistent to the photolysis or ozonolysis. For instance,
301 the expected tropospheric lifetime of hymexazol in a spring-summer day is 19.3 h at
302 non-polluted location ([O_3] = 75 ppb, [OH] = 2 × 10^6 molecule cm^{-3}) and 6.8 h at
303 polluted location ([O_3] = 90 ppb, [OH] = 8.8 × 10^6 molecule cm^{-3}). These values
304 revealed the importance of characterizing the degradation products due to its short
305 atmospheric life-time. The high OH reactivity is quite similar than obtained for other
306 pesticide compounds at non-polluted locations - 3.5 h for chlorpyrifos-methyl (Muñoz
307 et al., 2011a), 4 h for diazinon (Muñoz et al., 2011b) , 8.5 h for trifluralin (Le Person et
308 al., 2007), 4.9 h for dichlorvos (Feigenbrugel et al., 2006) and 20 h for propachlor
309 (Muñoz et al., 2012).

310 The detection of several structurally defined products has allowed understanding
311 of the degradation process, showing some differences respect to other aromatic,
312 heterocycles, or pesticides compounds. As opposite of other aromatic compounds,
313 isoxazole ring compounds present no significant differences between the absence and
314 the presence of NO_x, in relation with the chemical composition of degradation products
315 formed. The analysis of chemical composition and their rate-formation also indicates

316 that isoxazole derivatives probably are a relevant source of nitrogen compounds, ozone,
317 and multi-oxygenated compounds, but the formation of secondary particulate matter is
318 reduced. The formation of nitrogen oxides, nitric acid, PAN or multi-oxygenated
319 compounds, is important because they play a significant role of atmospheric chemistry.

320 ## ACKNOWLEDGMENTS

321 The authors wish to thank the EUPHORE staff and J.T.B. The authors wish to
322 acknowledge Ministerio de Ciencia y Tecnología for IMPESTAT (CGL2010-
323 18474/CLI) and the European Community's Seventh Framework Program under the
324 grant agreement no. 228335 (Eurochamp2). The Fundación CEAM is partly supported
325 by Generalitat Valenciana, and the projects GRACCIE (Consolider-Ingenio 2010) and
326 FEEDBACKS (Prometeo - Generalitat Valenciana). EUPHORE instrumentation is
327 partly funded by the Spanish Ministry of Science and Innovation, through
328 INNPLANTA project: PCT-440000-2010-003.

329 ## REFERENCES

330 Atkinson, R., Aschmann, S.M., Carter,W.P.L. 1983. Kinetics of the reactions of
331 O_3 and OH radicals with furan and thiophene at 298 ± 2 K. Int. J. Chem. Kinet. 15, 51-
332 61.

333 Atkinson, R.; S.M Aschmann.; A.M. Winer,; W.P.L Carter. 1984. Rate constants
334 for the gas phase reactions of OH radicals and O_3 with pyrrole at 295 ± 1 K and
335 atmospheric pressure. Atmos. Environ. 18, 2105-2107.

336 Atkinson, R.; Guicherit, R.; Hites, R.A.; Palm, W.U.; Seiber, J.N.; de Voogt, P.
337 1999. Transformations of pesticides in the atmosphere: A state of the art. Water, Air,
338 Soil Pollut. 115, 219-243.

Baltaretu, C.O.; Lichtman, E.I.; Hadler, A.B.; Elrod, M.J. 2009. Primary Atmospheric Oxidation Mechanism for Toluene. J. Phys. Chem. A 113, 221–230.

Bejan, I.; Abd El Aal, Y.; Barnes, I.; Benter, T.; Bohn, B.; Wiesen, P.; Kleffmann, J. 2006. The photolysis of ortho-nitrophenols: a new gas phase source of HONO. Phys. Chem. Chem. Phys 8, 2028–2035.

Bierbach, A.; Barnes, I.; Becker, K.H. 1992. Rate coefficients for the gas-phase reactions of hydroxyl radicals with furan, 2-methylfuran, 2-ethylfuran and 2,5-dimethylfuran at 300 ± 2 K. Atmos. Environ. 26, 813-817

Borrás, E.; Tortajada-Genaro, L.A. 2012a. Secondary organic aerosol formation from the photo-oxidation of benzene. Atmos. Environ. 47, 154-163.

Borrás, E.; Tortajada-Genaro, L.A. 2012b. Determination of oxygenated compounds in secondary organic aerosol from isoprene and toluene smog chamber experiments. Intern. J. Environ. Anal. Chem. 92, 110–124.

Cabañas, B.; Baeza, M.T.; Salgado, S.; Martín, P.; Taccone, R.; Martínez, E. 2004. Oxidation of Heterocycles in the Atmosphere: Kinetic Study of Their Reactions with NO_3 Radical. J. Phys. Chem. A 108, 10818-10823.

Dillon, T.J.; Tucceri, M.E.; Dulitz, K.; Horowitz, A.; Vereecken, L.; Crowley, J.N. 2012. Reaction of Hydroxyl Radicals with C_4H_5N (Pyrrole): Temperature and Pressure Dependent Rate Coefficients. J. Phys. Chem. A 116, 6051−6058.

Feigenbrugel, V,; Le Person, A,; Le Calvé, S.; Mellouki, A.; Muñoz, A.; Wirtz, K. 2006. Atmospheric fate of dichlorvos: photolysis and OH-initiated oxidation studies. Environ. Sci. Technol. 40, 850-857.

Finlayson-Pitts, B.J.; Pitts, J.N. Chemistry of the Upper and Lower Atmosphere: Theory, Experiments and Applications. Academic Press, San Diego, CA. 2000

363 FOCUS Working Group, Pesticides in Air: Considerations for Exposure
364 Assessment, European Union, Brussels, SANCO/10553/2006 Rev, June 2, 2008
365 Gomez Alvarez, E.; Borrás, E.; Viidanoja, J.; Hjorth, J. 2009. Unsaturated
366 dicarbonyl products from the OH-initiated photo-oxidation of furan, 2-methylfuran and
367 3-methylfuran. Atmos. Environ. 43, 1603–1612.
368 Kwok, E.R.C.; Atkison, R. 1995. Estimation of hydroxyl radical reaction rate
369 constant for gas-phase organic compounds using a structure-reactivity relationship: an
370 update. Atmos. Chem. 29, 1685-1695.
371 Le Person, A.; Mellouki, A.; Muñoz, A.; Borras, E.; Martin-Reviejo, M.; Wirtz,
372 K. 2007. Trifluralin: Photolysis under sunlight conditions and reaction with HO radicals.
373 Chemosphere 67, 376–383.
374 Mellouki, A.; Le Bras, G.; Sidebottom, H. 2003. Kinetics and Mechanisms of
375 the Oxidation of Oxygenated Organic Compounds in the Gas Phase. Chem. Rev. 103,
376 5077-5096.
377 Mereau, R., Rayez, M-T., Caralp, F., Rayez, J-C. 2003. Isomerisation reactions
378 of alkoxy radicals: theoretical study and structure–activity relationships. Phys. Chem.
379 Chem. Phys., 5, 4828–4833.
380 Muñoz, A.; Vera, T.; Sidebottom, H.; Mellouki, A.; Borrás, E.; Rodenas, M.;
381 Clemente, E.; Vázquez. M. 2011a. Studies on the Atmospheric Degradation of
382 Chlorpyrifos-Methyl. Environ. Sci. Technol. 45, 1880–1886.
383 Muñoz, A.; Le Person, A.; Le Calvé, S.; Mellouki, A.; Borrás, E.; Daële, V.;
384 Vera, T. 2011b. Studies on atmospheric degradation of diazinon in the EUPHORE
385 simulation chamber. Chemosphere 85, 724-730.

Muñoz, A.; Vera, T.; Sidebottom, H.; Ródenas, M.; Borrás, E.; Vázquez, M.; Raro, M.; Mellouki. 2012. A. Studies on the atmospheric fate of propachlor (2-chloro-N-isopropylacetanilide) in the gas-phase. Atmos. Environ. 49, 33-40.

Ng, N.L.; Kroll, J.H.; Chan, A.W.H.; Chhabra, P.S.; Flagan, R.C.; Seinfeld, J. H. 2007. Secondary organic aerosol formation from m-xylene, toluene, and benzene. Atmos. Chem. Phys. 7, 3909–3922.

Payne, P.A.; Williams, G.E. 1990. Hymexazol treatment of sugar-beet seed to control seedling disease caused by Pythium spp. and Aphanomyces cochlioides. Crop Protection 5, 371-377.

Van Den Berg, F.; Kubiak, R.; Benjey, W.G.; Majewski, M.S.; Yates, S.R.; Reeves, G.L.; Smelt, J.H.; Van Der Linden, A.M.A. 1999. Emission of pesticides into the air. Water, Air and Soil Pollut. 115, 195-218.

Vera, T.; Muñoz, A.; Rodenas, M.; Vázquez, M.; Borrás, E.; Marqués, M.; Mellouki, A.; Treacy, J.; Sidebottom, H. 2011. Atmospheric fate of hymexazol (5-methylisoxazol-3-ol): Simulation chamber studies. Atmos. Environ. 45, 3704-3710.

411 Table 1. Experimental conditions of atmospheric degradations.

412

Experiment Type	Solar radiation	Relative humidity	Aerosol seeds	Hymexazol ($\mu g\ m^{-3}$)	O_3 ($\mu g\ m^{-3}$)	H_2O_2 ($\mu g\ m^{-3}$)	HONO ($\mu g\ m^{-3} min^{-1}$)
Chamber background A	No	Dry	No	-	-	-	-
Chamber background B	Yes	Dry	No	-	-	-	-
Chamber background C	No	Dry	Yes	-	-	-	-
Hymexazol wall losses	No	Dry	No	2582	-	-	-
Photolysis	Yes	Dry	No	1821	-	-	-
Ozonolysis	No	Dry	No	2530	130	-	-
Photo-oxidation (absence NO_x)	Yes	Dry	No	3208	-	19850	-
Photo-oxidation (presence NO_x)	Yes	Dry	No	3053	-	-	3.8*
Photo-oxidation (presence NO_x)	Yes	Dry	No	2701	-	-	3.8*
Photo-oxidation (presence NO_x)	Yes	Dry	No	2871	-	-	3.8*

413 * HONO continuoulsy added

414

415

416

417

418

419

420

421

422

423

424

425

426

427

428

429

Table 2. Concentration of gas-products (μg m^{-3}). Values in parentheses indicate the reaction mass-based yields.

Experiment	O_3	HNO_3	NO_2	NO	HCOOH	PAN	HONO	HCHO	MG
Photolysis	82.6	< 1.3	35.2	< 0.4	19.6	< 9.9	< 2.9	< 1.2	< 5.9
	(49.1)	-	(22.5)	-	(11.4)	-	-	-	-
Ozonolysis	-	< 1.3	65.1	< 0.4	< 3.8	< 9.9	< 2.9	< 1.2	< 5.9
	-	-	(25)	-	-	-	-	-	-
Photo-oxidation	813.4	100	13.5	< 0.4	101.2	86.4	5.3	23.5	33.4
(NO_x absence)	(46.5)	(5.8)	(0.8)		(5.8)	(5.0)	(0.1)	(1.3)	(1.7)
Photo-oxidation	96.9	598.8	514.9	135.5	40.3	30.9	79.2	50.8	28.6
(high NO_x)	(4.7)	(29.2)	(34.4)	(13.9)	(2.3)	(0.8)	-	(2.9)	(1.6)

PAN: peroxyacetylnitrate, MG: methylglyoxal

454 Figure 1. Concentration profiles for main gas phase products from hymexazol photo-
455 oxidation: (a) NO_x-absence conditions and (b) NO_x-presence conditions.

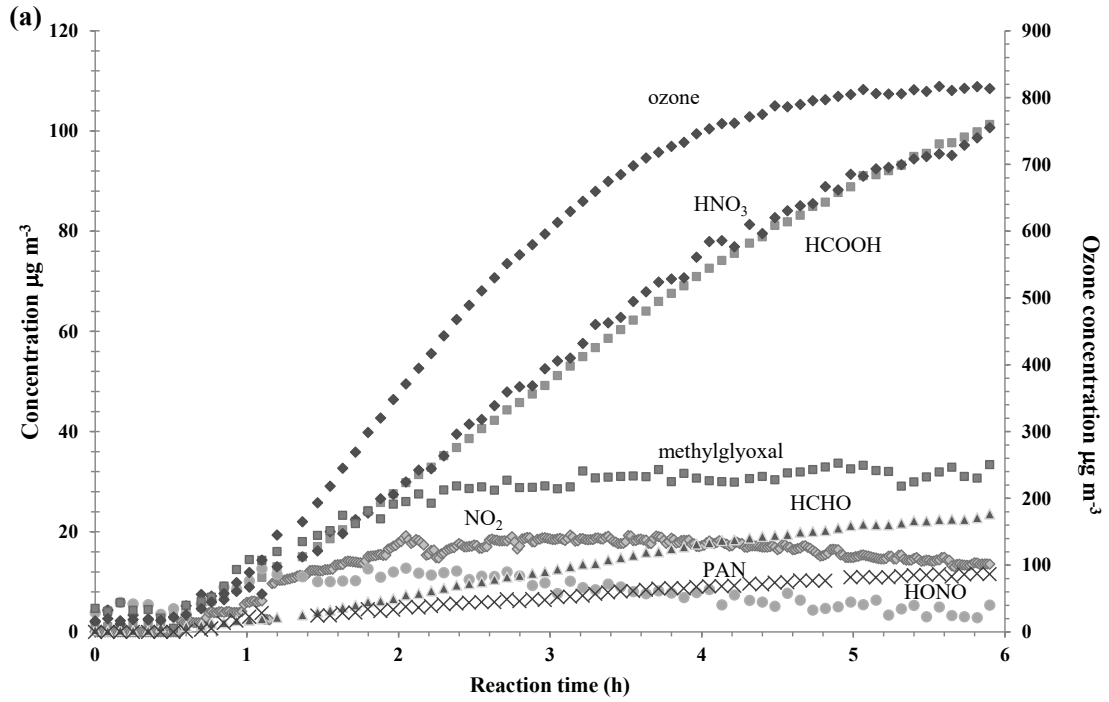

456

457

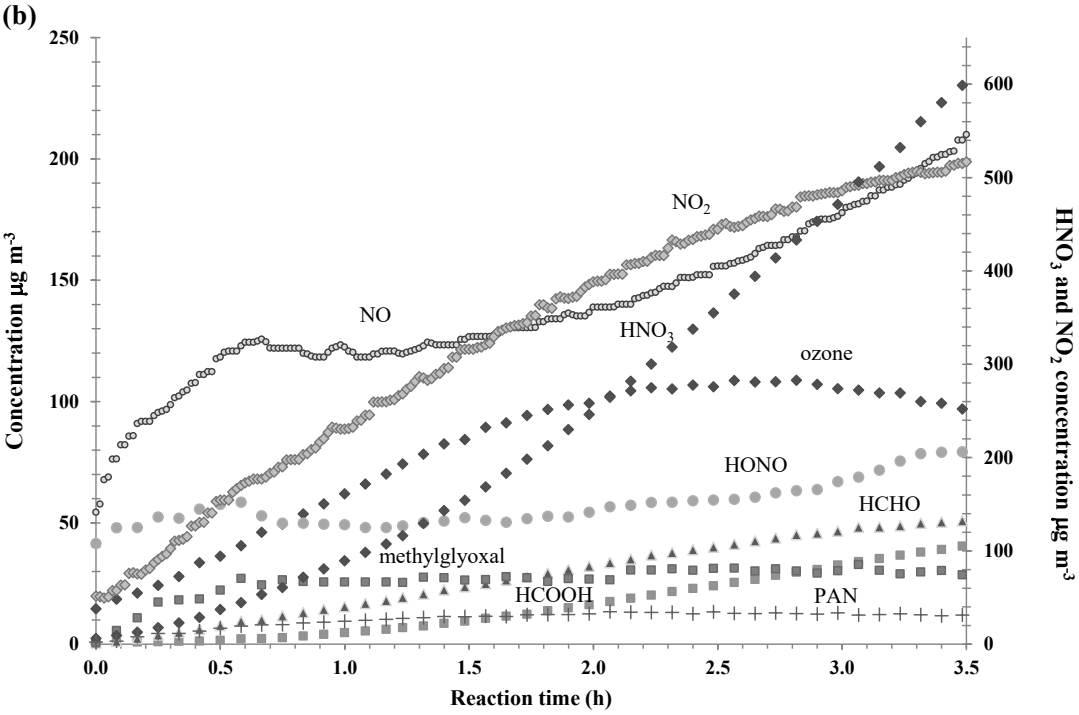

458

459

Figure 2. Concentration profiles for particle matter from hymexazol photo-oxidation: (a) NO_x-absence conditions and (b) NO_x-presence conditions. Inserts illustrate size distribution expressed as number of particles vs. diameter (nm), indicating the central particle size.

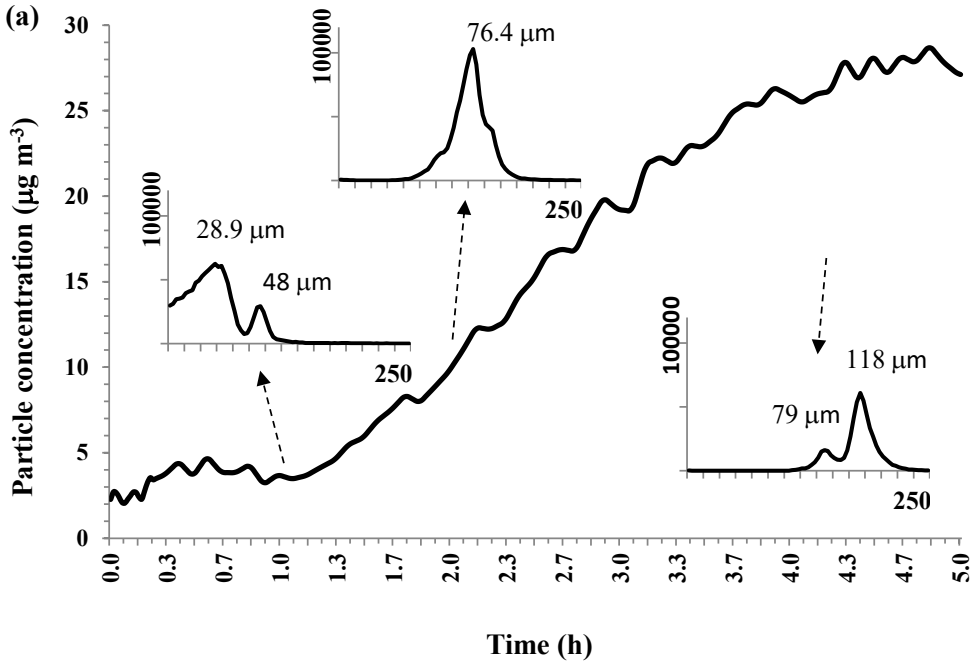

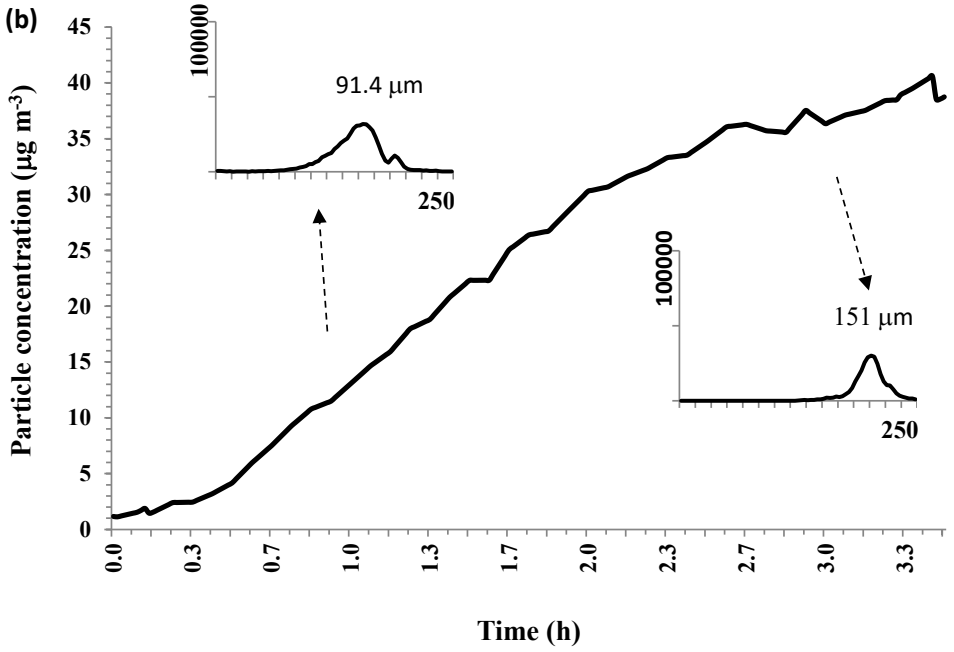

Figure 3. Extracted ion chromatogram (m/z=73 and m/z=181) from gaseous sample collected during NO_x-presence photo-oxidation.